Atmos. Meas. Tech. Discuss., 2, 119–151, 2009
www.atmos-meas-tech-discuss.net/2/119/2009/

Atmospheric Measurement Techniques Discussions

Atmospheric Measurement Techniques Discussions is the access reviewed discussion forum of *Atmospheric Measurement Techniques*

Chlorine activation by N_2O_5: simultaneous, in situ detection of $ClNO_2$ and N_2O_5 by chemical ionization mass spectrometry

J. P. Kercher[1], T. P. Riedel[1,2], and J. A. Thornton[1]

[1]Department of Atmospheric Sciences, University of Washington, Seattle, WA 98195, USA
[2]Department of Chemistry, University of Washington, Seattle, WA 98195, USA

Received: 2 December 2008 – Accepted: 7 December 2008 – Published: 14 January 2009

Correspondence to: J. A. Thornton (thornton@atmos.washington.edu)

Published by Copernicus Publications on behalf of the European Geosciences Union.

Abstract

We report a new method for the simultaneous in situ detection of nitryl chloride ($ClNO_2$) and dinitrogen pentoxide (N_2O_5) using chemical ionization mass spectrometry (CIMS). The technique relies on the formation and detection of iodide ion-molecule clusters, $I(ClNO_2)^-$ and $I(N_2O_5)^-$. The novel N_2O_5 detection scheme is direct. It does not suffer from high and variable chemical interferences, which are associated with the typical method of nitrate anion detection. We address the role of water vapor, electric field strength, and instrument zero determinations, which influence the overall sensitivity and detection limit of this method. For both species, the method demonstrates high sensitivity (>1 Hz/pptv), precision (~10% for 100 pptv in 1 s), and accuracy (~20%), the latter ultimately determined by the nitrogen dioxide (NO_2) cylinder calibration standard and characterization of inlet effects. For the typically low background signals (<10 Hz) and high selectivity, we estimate signal-to-noise (*S/N*) ratios of 2 for 1 pptv in 60 s averages, but uncertainty associated with the instrumental zero currently leads to an ultimate detection limit of ~5 pptv for both species. We validate our approach for the simultaneous in situ measurement of $ClNO_2$ and N_2O_5 while on board the Research Vessel (RV) Knorr as part of the ICEALOT 2008 Field Campaign.

1 Introduction

Human activities of industry, transportation, and agriculture account for ~75% of global nitrogen oxide ($NO_x \equiv NO+NO_2$) emissions, and these emissions are expected to be double the 1990 values in about a decade (van Aardenne et al., 1999; Yienger, 1999). NO_x plays a fundamental role in the troposphere's oxidizing capacity by regulating photochemical ozone production rates, and by partly controlling hydrogen oxide ($HO_x \equiv OH+HO_2$) and halogen oxide radical cycles (Logan, 1981). The regional and global scale impacts of anthropogenic NO_x emissions ultimately depend on its atmospheric lifetime, which is primarily controlled by nitric acid (HNO_3) formation during the

AMTD

2, 119–151, 2009

daytime,

$$NO_2 + OH + M \rightarrow HNO_3M \quad \text{(R1)}$$

and by homogeneous and heterogeneous reactions of the nitrate radical (NO_3) and dinitrogen pentoxide (N_2O_5) at night (R2–R7).

$$NO_2 + O_3 \rightarrow NO_3 + O_2 \quad \text{(R2)}$$

$$NO_2 + NO_3 \rightleftarrows N_2O_5 \quad \text{(R3)}$$

$$NO_3 + VOC \rightarrow \text{products} \quad \text{(R4)}$$

$$NO_3 + \text{particles} \rightarrow \text{products} \quad \text{(R5)}$$

$$N_2O_5 + \text{particles} \xrightarrow{H_2O} 2HNO_3 \quad \text{(R6)}$$

$$N_2O_5 + \text{particles} \xrightarrow{H^+, Cl^-_{aq}} ClNO_2 + HNO_3 \quad \text{(R7)}$$

Nocturnal processing of NO_3 and N_2O_5 has been estimated to remove approximately half of NO_x, globally, and is a significant loss process for total odd-oxygen ($O_x \equiv O_3 + NO_2$) (Brown et al., 2006; Dentener and Crutzen, 1993; Evans and Jacob, 2005). The chemistry involves reactions of NO_3 with a suite of diverse volatile organic compounds (VOC), and heterogeneous reactions of both NO_3 and N_2O_5 with aerosol particles (Atkinson, 2000; Jacob, 2000; Mentel et al., 1996; Noxon et al., 1980; Platt and Heintz, 1994; Wayne et al., 1991). The branching between various pathways is strongly dependent on temperature, NO_x, hydrocarbons, particle composition, and vertical mixing (Ayers and Simpson, 2006; Brown et al., 2007; Stutz et al., 2004); as such, several aspects of this chemistry remain uncertain.

Laboratory studies have conclusively shown that the reaction of N_2O_5 on chloride containing solutions and solids yields nitryl chloride ($ClNO_2$), a photo-labile chlorine atom source (Behnke et al., 1997; Finlayson-Pitts et al., 1989; Thornton and Abbatt,

AMTD
2, 119–151, 2009

2005). The relative branching between Reactions (R6) and (R7) for use in atmospheric chemistry models has essentially remained unconstrained due to a lack of in situ observations of $ClNO_2$. $ClNO_2$ is fairly unreactive at night such that given sustained production via (R7), its concentration can increase throughout nighttime. A recent theoretical study predicted $ClNO_2$ mixing ratios of up to 50 parts per trillion by volume (pptv) in polluted regions (e.g. the Long Island Sound) (Pechtl and von Glasow, 2007).

During the daytime, $ClNO_2$ undergoes photolysis by UV-VIS radiation to generate chlorine atoms and NO_2 with a clear-sky lifetime of order 30–60 min depending on season and location.

$$ClNO_2 + h\nu \rightarrow Cl + NO_2 \quad \text{(R8)}$$

The importance of the reaction sequence (R7)–(R8) is two-fold. First, in a NO_x-laden air mass, the photodissociation of $ClNO_2$ can initiate photochemical ozone production earlier than would otherwise occur, ultimately increasing the integral amount of ozone produced. This effect is due to the fact that reaction R8 goes to completion within an hour or two after sunrise, liberating chlorine atoms which react with hydrocarbons up to 10–100 times faster than does the hydroxyl radical (OH). While Cl-atoms have not been directly observed, labile sources in addition to $ClNO_2$, such as Cl_2, have been observed (Spicer et al., 1998). Regionally averaged Cl abundances have been inferred from observational analyses of hydrocarbons (Arsene et al., 2007; Cavender et al., 2008), but due to the limited spatial and temporal coverage of such measurements, the global Cl-atom source term remains largely unconstrained (Platt et al., 2004). Second, since $ClNO_2$ is not a terminal NO_x sink, production via N_2O_5 heterogeneous reaction represents a reduction, by as much as 50%, in the amount of NO_x removed during night by NO_3 and N_2O_5 chemistry, effectively enhancing the NO_x-lifetime because reaction R8 ultimately returns one NO_x.

Tropospheric N_2O_5 mixing ratios can vary from less than 10 pptv to above 1000 pptv (Aldener et al., 2006; Ayers and Simpson, 2006; Simpson, 2003). The tropospheric N_2O_5 abundance was first inferred from long-path differential optical absorption spectroscopy (DOAS) measurements of NO_3 together with measurements of NO_2 and an

assumption that NO_3, NO_2 and N_2O_5 are related by the equilibrium shown in (R3) (Heintz et al., 1996; Smith et al., 1995; Stutz et al., 2004). Recently, multiple groups have demonstrated a difference method for in situ N_2O_5 observations, where N_2O_5 is thermally decomposed to NO_3, which is then detected by cavity ring-down spectroscopy (CaRDS) or laser-induced fluorescence (Geyer et al., 1999; Simpson, 2003; Wood et al., 2003). The contribution of ambient NO_3, which is generally small, is subtracted from the total signal measured after N_2O_5 thermal decomposition. The sum of N_2O_5 and NO_3 can also be measured as the nitrate anion, NO_3^-, by chemical ionization mass spectrometry (CIMS) using the iodide reagent ion (I^-). Indeed, this particular CIMS approach has been employed in numerous laboratory studies (Huey et al., 1995; Thornton et al., 2003) and has been demonstrated as a potential in situ method for N_2O_5 detection (Huey, 2007; Slusher et al., 2004).

Recently, we showed that $ClNO_2$ could be sensitively and selectively detected by I^- CIMS (McNeill et al., 2006), leading to the first in situ detection of $ClNO_2$ in the polluted Gulf of Mexico (Osthoff et al., 2008). Here, we describe this technique further, and demonstrate a new method that allows the detection of both N_2O_5 and $ClNO_2$ at pptv mixing ratios using the same instrument. We illustrate the instrument's performance during the initial phase of the International Chemistry Experiment in the Arctic Lower Troposphere (ICEALOT), a recent ship-based research cruise that took place March–April 2008. The unique aspects of this method include a combination of high sensitivity (~1 Hz $pptv^{-1}$), low background noise (<10 Hz), and chemical selectivity for both $ClNO_2$ and N_2O_5. The N_2O_5 measurement is direct, i.e. the signal does not include contributions from NO_3, and it does not suffer from high and variable chemical interferences which affect the NO_3^--based detection method. Essentially, the method provides the ability to simultaneously monitor both the reactant (N_2O_5) and product ($ClNO_2$) of an atmospheric heterogeneous process, in situ, with a fixed relative calibration.

AMTD
2, 119–151, 2009

2 Instrument description

The University of Washington chemical ionization mass spectrometer (UW-CIMS), has previously been described (Wolfe et al., 2007), and is similar in concept to other field-deployable CIMS instruments (Slusher et al., 2004; Veres et al., 2008). In this section, we briefly discuss the major components and operation of the UW-CIMS with special attention paid to features allowing for detection of N_2O_5 and $ClNO_2$. A schematic of the UW-CIMS illustrating the four major components is shown in Fig. 1. These regions are: 1) ion-molecule reaction region, 2) collisional dissociation chamber, 3) octupole ion guide, 4) quadrupole mass spectrometer and electron multiplier.

2.1 Ion Molecule Reaction Region (IMR)

Ambient air, sampled by a rotary vane pump, passes through a critical orifice into a 4 cm OD electrically isolated stainless steel flow tube that serves as the IMR region. The orifice and vacuum pump maintain a constant volumetric flow rate of 2 standard liters per minute (slpm) through the sampling orifice, and a pressure of 60 torr. A commercial ^{210}Po radioactive ion source (alpha-emitter, 10 mCu), oriented perpendicular to the main sample flow axis, is located along the reaction flow tube ~1 cm downstream of the sampling orifice. Iodide anions (I^-) are introduced to the sample stream by passing a 2.5 slpm flow of ultra high purity (UHP) N_2 that contains a trace amount of methyl iodide (CH_3I) through the ^{210}Po ion source. Neutral molecules in air react with iodide anions for ~70 ms before exiting the IMR region.

2.2 Collisional Dissociation Chamber (CDC)

A fraction (~10%) of the ion-molecule reaction mixture is sampled from the IMR into the collsional declustering region (CDC) by means of a second orifice biased to −65 V relative to ground. A 7 liters per second (lps) molecular drag pump is used to drop the pressure from 60 torr in the IMR to 1.5 torr in the CDC. The CDC is comprised of

AMTD
2, 119–151, 2009

a series of 4 static lenses. The lenses are 2 mm thick, 4 cm OD, 1 cm ID, stainless steel discs that are spaced 6 mm from each other, and from the two orifice plates, which serve as the entrance and exit to/from the CDC. The front pair of lenses are biased to −45 V and the rear pair are biased to −25 V. The third orifice plate, which separates the CDC from the high vacuum chamber, is biased to −5.1 V to create a net electric field of −20 V/cm at 1.5 torr. This field strength is less than that typically used by our group and others to detect acyl peroxy nitrates by I^- CIMS (Wolfe et al., 2007). As discussed below, this lower field strength allows for the simultaneous detection of N_2O_5 and $ClNO_2$.

2.3 Octupole ion guide

Ions are focused through the CDC orifice plate into the fore chamber of a differentially pumped stainless steel high vacuum region. The fore chamber, pumped by a 250 lps turbomolecular pump, is maintained at 3 mtorr. Ions are focused into a narrow beam and transmitted into the quadrupole region by a custom RF-only octupole ion guide. The 4 cm long, 2 cm OD octupole ion guide, based on the designs of Tanner et al. at Georgia Tech (Tanner, D. J., personal communication), is driven by a compact RF-only power supply (2.2 MHz, 220 V p-p) designed at the University of Washington. The octupole is mounted on a fourth, and final orifice plate, which drops the pressure from 3 mtorr to 2×10^{-5} torr by means of a second 250 lps turbomolecular pump. The ion beam is focused through the orifice into the quadrupole mass selector. The two turbomolecular pumps are backed by molecular drag pumps, in turn backed by the same rotary vane pump which maintains the IMR region pressure and flows.

2.4 Quadrupole Mass Selection (QMS) and detection

Ions transmitted through the final orifice are mass selected using a quadrupole mass selector (QMS) from Extrel Inc. housed in a high vacuum region held at 2×10^{-5} torr. The quadrupole has 19 mm OD rods equipped with RF-only pre and post filters, and is

AMTD
2, 119–151, 2009

driven by a 300 W, 1.2 MHz RF/DC power supply. The quadrupole rods are housed in a perforated stainless steel tube capped with entrance and exit lenses, and are followed by an off-axis electron multiplier detector with dynode from Extrel Inc. An MTS-100 preamp is used to convert the output pulses of the multiplier into TTL. The multiplier, preamp, and ion optics, including orifice plates and CDC lenses, are powered or biased using pre-packaged Extrel Inc. power supplies.

2.5 Instrument control and data acquisition

Diagnostics monitoring and instrument control are handled via a 32-bit, 32 kHz analog-to-digital converter controlled by custom LabVIEW software on a custom rack-mounted PC. Typically, 4–20 individual mass-to-charge (*m/z*) ratios are monitored continuously while sampling ambient air. The signal at an *m/z* is determined by sending a mass command voltage to the RF/DC quadrupole power supply, counting the TTL preamp output for a set period per *m/z*, typically 80–250 ms, then moving to the next *m/z*. Depending on the number of individual *m/z* to monitor, this scheme leads to sampling frequencies ranging from 0.2 to 3 Hz per *m/z*.

3 Ion chemistry

Neglecting the role of water vapor in the ion-molecule reaction region, the ion chemistry for the detection of both N_2O_5 and $ClNO_2$ proceeds through two channels: dissociative charge transfer (R9 and R12) and cluster formation (R11 and R13). With the exception of reaction R11, the reaction channels described below have been demonstrated and used previously, primarily for laboratory studies (Huey, 2007; McNeill et al., 2006; Thornton et al., 2003).

$$I^- + N_2O_5 \rightarrow NO_3^- + INO_2 \quad \text{(R9)}$$

$$I^- + NO_3 \rightarrow NO_3^- + I \quad \text{(R10)}$$

$$I^- + N_2O_5 \rightarrow I(N_2O_5)^- \quad \text{(R11)}$$

$$I^- + ClNO_2 \rightarrow ICl^- + INO_2 \quad \text{(R12)}$$

$$I^- + ClNO_2 \rightarrow I(ClNO_2)^- \quad \text{(R13)}$$

Figure 2 shows a sample ion time trace obtained in the laboratory for the four products discussed above, under sampling conditions which have been optimized for the detection of the cluster anions. Initially, N_2O_5 (750 pptv) in a 2.5 slpm flow of dry N_2 was sampled directly into the UW-CIMS. The NO_3^- and $I(N_2O_5)^-$ anions are observed in a 3:1 ratio. The boxed regions highlight the times when the N_2O_5 flow passed over a wet sodium chloride (NaCl) salt bed prior to sampling by the UW-CIMS. In addition to NO_3^- and $I(N_2O_5)^-$, ICl^- and $I(ClNO_2)^-$ are observed during these times, with the cluster anion representing 80% of the total nitryl chloride signal. The factors governing the observed branching between reactive charge transfer and cluster formation for both $ClNO_2$ and N_2O_5 are discussed below.

4 Sensitivity and selectivity

4.1 Calibrations

The true instrument sensitivity is a function of conditions both internal and external to the CIMS instrument. For example, ion transmission efficiency is affected on the short term, of minutes-hours, by temperature-dependent drifts in power supply outputs which affect static and RF potentials; and on the long term, as electron multipliers lose gain and detection efficiency decreases over the course of months to years. Air mass changes or diurnal boundary layer expansion and contraction can lead to changes in the partial pressure of H_2O which impacts ion chemistry. We routinely add known mixing ratios of N_2O_5 and $ClNO_2$ to the sample flow to capture such changes in instrument sensitivity. This procedure provides a calibration factor, C_f, in units of count rate per

AMTD
2, 119–151, 2009

pptv (Hz/pptv) of N_2O_5 or $ClNO_2$ sampled, that is then interpolated onto the measurement time base and used to convert instantaneous count rates into absolute mixing ratios.

Well-quantified, highly reproducible, and commercially available sources of N_2O_5 and $ClNO_2$ do not exist. We use a combination of generation and quantification methods to develop confidence in the calibration sources we apply in the field. During ICEALOT 2008, N_2O_5 was delivered to the sampling inlet for calibration purposes, one to two times per day, by passing a small flow of N_2 over pure, solid N_2O_5 maintained at −75°C. Two types of additions were performed: one while overflowing the inlet with dry zero air, and one by adding the N_2O_5 directly to moist ambient air. The NOAA CaRDS instrument, sampling from the same inlet manifold as the UW-CIMS, used these additions primarily to assess inlet transmission. For the purpose of this campaign, a goal of which was to test our N_2O_5 detection capability, we relied on the NOAA CaRDS instrument to determine the N_2O_5 concentration being delivered to the UW-CIMS inlet during these calibrations. We then used this known N_2O_5 concentration, typically a single value between 1–5 ppbv, to generate a C_f for the UW-CIMS based on the observed signal at the $I(N_2O_5)^-$ *m/z*. Figure 3 shows the resulting plots of signal (Hz) versus N_2O_5 mixing ratio sampled in relatively dry air (RH~20%). The slope of linear least squares fit to the data yield a calibration factor of 0.75 Hz/pptv. An example of a calibration performed during the deployment is shown and discussed in the section on field performance.

The difficulty with using the equilibrium vapor pressure over solid N_2O_5 as a CIMS calibration source is that the N_2O_5 solid is subject to contamination, which results in unknown changes in the vapor pressure on a weekly, if not daily timescale. Without an absolute calibration, such as the known NO_3 absorption cross-section available to cavity ring-down techniques, abrupt (or gradual) changes in trap-output are undesirable. Furthermore, temperature control of the cold-bath must also be precise given that the vapor pressure in equilibrium with the solid changes by 30–50% per degree K, and routine calibrations require dry ice or liquid nitrogen to maintain the trap cold-bath

AMTD
2, 119–151, 2009

which is not ideal for long field deployments.

Our preferred method for independent calibration of the UW-CIMS to N_2O_5 in future field deployments is to deliver the output from a custom PFA-Teflon flow reactor in which N_2O_5 is continuously produced from the well known reaction of NO_2 with O_3, i.e. Reactions (R2)–(R3). The N_2O_5 source is described in detail elsewhere (Bertram et al., 2009). Briefly, the reaction is performed under excess NO_2 delivered at 2–10 standard cubic cm per minute (sccm) from a NIST-traceable cylinder of 10 ppm NO_2 in a balance of N_2 through a stainless steel mesh to scrub HNO_3 prior to entry into the flow reactor. The NO_2 mixing ratio in the reactor volume is typically of order 1 ppm. O_3 mixing ratios of 150–200 ppbv are generated by passing 50 sccm of UHP zero air through a custom stainless steel chamber illuminated by a Hg pen-ray lamp. The ozone and NO_2 mix and react for 2 min prior to dilution into the sample flow. After a 20:1 dilution, the mixing ratio of N_2O_5 is between 1 and 10 ppbv, depending on the NO_2 flow. Based on recent laboratory and field tests, the output is constant to within 5% over several hours of continuous operation and accurate to within 20% (see more details below).

We calibrate to $ClNO_2$ by passing a dry N_2 flow containing a known mixing ratio of N_2O_5 over a wet NaCl bed, which is dispersed along the inner walls of a 20 cm length of 13 mm OD tubing. The mixing ratio of $ClNO_2$ eluting from the salt bed is calculated from the observed amount of N_2O_5 lost when passing through the salt bed and the known $ClNO_2$ yield (100%) from the reaction of N_2O_5 on NaCl (Behnke et al., 1997; Finlayson-Pitts et al., 1989; McNeill et al., 2006). The inset of Fig. 3 shows the $I(ClNO_2)^-$ signal in response to passing 1.0 and 1.5 ppbv N_2O_5 in ambient air (RH~20%) over a wet NaCl bed. The resulting binned signal is plotted versus the calculated $ClNO_2$ concentration. The slope yields 0.9 Hz/pptv for a calibration factor under relatively dry sampling conditions.

4.2 Factors affecting sensitivity

Fundamentally, the sensitivity and linearity of a CIMS method depends on the rate of product ion formation, the ion-molecule reaction time, and the ion transmission and

AMTD
2, 119–151, 2009

detection efficiencies. Ideally, the product ion formation rate is maximized by using high densities of a reagent ion which reacts at the collision limit with the analyte of interest to produce detectable count rates (Hz) of a unique product ion in a short interaction time. A short interaction time ensures a small extent of reaction and thus that the product ion abundance remains linearly proportional to the analyte concentration. For a more complete discussion of these issues, we refer the reader elsewhere (Harrison, 1983). Here, we focus on two factors which affect the sensitivity of our I^- CIMS to $ClNO_2$ and N_2O_5 via the iodide cluster channels (R11 and R13): water vapor mediated cluster formation and collisional dissociation in the CDC.

In sampling humid ambient air, iodide ions form clusters containing one or more water molecules, as do many of the analyte ions produced during the chemical ionization process. The formation of such complexes can enhance sensitivity by stabilizing reactive complexes, or, as is more often the case, such complexes can degrade sensitivity by reducing the reactivity of the reagent ion and/or by distributing the analyte ion of interest among several *m/z* thus decreasing the signal-to-noise (*S/N*). For this latter reason, a number of CIMS instruments employ a CDC to increase the *S/N*, by collapsing the analyte ion water cluster distribution into a single *m/z* representative of the parent ion mass. We illustrate below that both aspects are important.

4.2.1 Water vapor mediated cluster formation

Figure 4 shows the water vapor dependence of the $I(ClNO_2)^-$ and $I(N_2O_5)^-$ signals. To obtain this data, a constant mixing ratio of N_2O_5 and $ClNO_2$ were delivered to the UW-CIMS inlet as described below, while a humidified flow of N_2 was delivered directly to the IMR region via a separate length of tubing and orifice so that the results were not affected by humidity-dependent losses of N_2O_5 on the inlet tubing walls. The experiments were conducted with a typical CDC electric field strength of −40 V/cm (at 1.5 torr) that we use to simultaneously detect acyl peroxy nitrates, N_2O_5, and $ClNO_2$ in the field. The signals at both the N_2O_5 and $ClNO_2$ iodide clusters increase rapidly at low water concentrations and become independent of water vapor at approximately

0.3 torr water vapor pressure, P_{H_2O}, in the IMR region. Due to the moist salt bed used to produce $ClNO_2$, we were unable to achieve P_{H_2O}<0.1 torr in the IMR. Clearly, the formation of the N_2O_5 and $ClNO_2$ clusters is facilitated by water vapor implying that the $I(H_2O)^-$ cluster likely becomes an important additional reagent ion for production of $I(ClNO_2)^-$ and $I(N_2O_5)^-$

$$I(H_2O)^- + N_2O_5 \rightarrow I(N_2O_5)^- + H_2O \quad \text{(R14)}$$

$$I(H_2O)^- + ClNO_2 \rightarrow I(ClNO_2)^- + H_2O \quad \text{(R15)}$$

The behavior observed here for the N_2O_5 and $ClNO_2$ iodide clusters is remarkably similar to that exhibited by acyl peroxy radicals (Slusher et al., 2004). Under minimal declustering, i.e. E<−5 V/cm in the CDC, the ratio of I^- to $I(H_2O)^-$ signals is approximately 1:1 to 1:2. Higher order water clusters, such as $I(H_2O)_2^-$ and $I(H_2O)_3^-$, are detected, but are less than 25% and 10%, respectively, of the $I(H_2O)^-$ cluster signal. Thus, we presume that both I^- and $I(H_2O)^-$ are the most important reagent ions.

4.2.2 Collisional dissociation in the CDC

While the sensitivity to $ClNO_2$ and N_2O_5 at their respective iodide clusters is enhanced by the presence of water vapor, it is degraded by collisional dissociation in the CDC. Thus, we strike a balance in the operation of the CDC. The CDC electric field must be strong enough to dissociate water molecules associated with the analyte ions of interest to maintain a high *S/N* at the cluster-ion *m/z*. However, the field strength must be weak enough to allow the survival of the $I(ClNO_2)^-$ and $I(N_2O_5)^-$ clusters. In practice, there are often other species of interest for detection, such as acyl peroxy nitrates, the product ions of which may cluster with water more strongly than the iodide clusters of N_2O_5 and $ClNO_2$. Thus, the chosen CDC electric field strength usually does not favor maximum sensitivity to N_2O_5 and $ClNO_2$ via their iodide clusters.

The overall sensitivity and detection limit for a particular species is improved by producing a single ion for detection. By knowing the branching ratio between the reactive

charge transfer and cluster ion formation, the sensitivity and detection limit of the CIMS can be further optimized. To obtain an estimate of the branching between (R9) and (R11), and between (R12) and (R13) in the IMR at 60 torr, we examined the ratios of $I(ClNO_2)^-$ to ICl^- signals and of $I(N_2O_5)^-$ to NO_3^- signals as a function of electric field strength in the CDC. As the cluster product ions can be dissociated in the CDC, the relative signals detected after the CDC provide only lower limits to the true branching. With relatively moist N_2 sample or ion source flows, $I(ClNO_2)^-$ approaches ~80% of the total nitryl chloride signal $\{I(ClNO_2)^- + ICl^-\}$ while $I(N_2O_5)^-$ approaches up to ~50% of the total measured N_2O_5 signal $\{I(N_2O_5)^- + NO_3^- + NO_3(H_2O)^-\}$ as the CDC field strength is lowered to a few V/cm. The IMR pressure also likely affects the absolute branching given that the cluster channels are probably enhanced by third-body stabilization of the complexes. This issue deserves further study.

4.3 Specificity and instrumental zero determinations

In a complex matrix such as air, signal at some *m/z* cannot always be uniquely attributed to a specific compound. Chemical ionization provides a degree of specificity given that many possible ion-molecule reactions are either kinetically or thermodynamically prohibited from occurring. Thus, the appropriate choice of a reagent ion can greatly improve specificity. N_2O_5 and $ClNO_2$ also have certain chemical properties which can be utilized to enhance the inherent specificity of the CIMS method. First, both N_2O_5 and $ClNO_2$ thermally decompose around 425 K (Zhu and Lin, 2004). Second, at temperatures near 298 K, N_2O_5 exists in a dynamic equilibrium with NO_3 and NO_2. NO_3 reacts rapidly with NO to form NO_2

$$NO_3 + NO \rightarrow 2NO_2 \quad \text{(R16)}$$

Thus, addition of high concentrations of NO to sample air near room temperature should effectively titrate both N_2O_5 and NO_3 from the sample air (Fuchs et al., 2008). Third, chlorine has two abundant isotopes, ^{35}Cl and ^{37}Cl, naturally present at ~3:1, respectively. Thus, the $I(ClNO_2)^-$ cluster will appear at both 207.9 and 209.9 *m/z* in a

ratio that should match the natural isotopic abundance for chlorine. We use all of these qualities to ensure specificity in the N_2O_5 and $ClNO_2$ measurements. We assume that it is highly unlikely there exists chemical species that have *m/z* identical to N_2O_5 and $ClNO_2$, that cluster with the iodide ion, and that have the same chemical properties described above. Recent field tests suggest this assumption is valid.

To account for sources of signal at the $I(N_2O_5)^-$ and the $I(ClNO_2)^-$ *m/z* that are not due to N_2O_5 or $ClNO_2$, i.e. sources of background noise, we perform routine "zero" determinations in which N_2O_5 and $ClNO_2$ are scrubbed from ambient air and the residual signal is recorded. This background signal has two main sources: internal electronic noise and interferences, the latter of which are ions having *m/z* within the mass resolution of the *m/z* of the N_2O_5 and $ClNO_2$ iodide clusters. Our zero determinations include both short additions of high concentrations of NO (~1 ppm) to the sampling manifold to titrate N_2O_5, and sampling ambient air through a 30 cm long, 13 mm OD stainless steel tube filled with stainless steel wool and heated to 450 K. The air exiting the hot metal tube passes through a 20 cm length of 6 mm OD tubing and thus likely cools back to near ambient temperature prior to entry into the UW-CIMS. This latter method, with its high surface area of hot metal, efficiently scrubs NO_3 and Cl-atoms released by thermal decomposition of N_2O_5 and $ClNO_2$ whereas the NO addition will only scrub N_2O_5.

Instrument zeros performed through a hot metal thermal dissociation tube are simple, but must be carefully examined. For example, it is possible that an interfering species is also lost in the hot metal tube or that the composition of the air is significantly changed to affect the overall sensitivity. Both scenarios lead to an uncertainty in the true background. We have observed that the P_{H_2O} in the IMR is routinely lower during zero determinations than during ambient sampling, implying a different sensitivity during zero determinations (Fig. 4). To account for such sensitivity differences, we use $I(H_2O)^-$ and $I(H_2O)_2^-$ signals as indicators of P_{H_2O} and the sensitivity behavior shown in Fig. 4 to scale our measured background signal accordingly. This leads to an average background of 3±2 pptv for both N_2O_5 and $ClNO_2$.

AMTD
2, 119–151, 2009

4.4 Detection limits

The lowest concentration that gives rise to a signal which can be statistically differentiated from the instrumental background is termed the detection limit. It is a function of the instrumental sensitivity, background noise, and averaging time. A useful threshold for a statistical definition of a detection limit is the concentration at which the signal-to-noise ratio (*S/N*) is 2. Discrete ion counting follows Poisson statistics, thus the expected random variation about a mean count rate goes as the square root of the count rate. The signal-to-noise ratio can be calculated via

$$\frac{S}{N} = \frac{C_f [X] t}{\sqrt{C_f [X] t + 2Bt}} \quad (1)$$

where the numerator provides the total number of counts produced during a given integration period, t, while sampling air with a mixing ratio, $[X]$, of N_2O_5 or $ClNO_2$, and with a calibration factor, C_f. The denominator represents the total noise associated with such a measurement which comes from the scatter about the sum of the count rate associated with the signal and the underlying background count rate, B.

Under moist ambient conditions at Earth's surface, i.e. RH>50% and T>280 K, the C_f for N_2O_5 and $ClNO_2$ at the iodide clusters are 1.1 and 1.3 Hz/pptv, respectively, and the background count rates are 2 and 3 Hz, respectively. These parameters and Eq. (1) yield detection limits for N_2O_5 and $ClNO_2$ of 11 and 13 pptv for a one second measurement. These values improve with the square root of the averaging time to <2 pptv for a 1-min average. However, there is a limit to which time averaging can improve the *S/N*. The ability to distinguish signal from the background depends on the uncertainty in the background value which can be approximated as the point-to-point variation in the values determined by individual zero determinations as described above. During a recent field campaign the 1σ variation in the background count rate measurements was 2.5 Hz for N_2O_5 and $ClNO_2$, respectively, which is equivalent to 2.3 and 2.0 pptv using the above C_f.

AMTD
2, 119–151, 2009

4.5 Accuracy and precision

Ultimately, we expect the accuracy of our reported N_2O_5 and $ClNO_2$ mixing ratios will be largely determined by uncertainty in the NO_2 cylinder and O_3 concentration measurement. We compared the observed changes in O_3 mixing ratios eluting from the continuous-flow N_2O_5 source, described above, to those predicted by a time-dependent chemical model of the source for a range of initial NO_2 mixing ratios. The output of our continuous-flow N_2O_5 source agrees with the predicted values to within the 20% uncertainty in the NO_2 cylinder concentration, O_3 mixing ratio measurement, and plug-flow estimated reaction time. Thus, for hourly or longer time averages, across which we will have a well-calibrated knowledge of instrument sensitivity and background, we can report an accuracy of 20% for $ClNO_2$ and N_2O_5 mixing ratios well above 5 pptv. On shorter timescales, we rely on normalization of ion count rates to the total I^- and $I(H_2O)_2^-$ clusters to capture changes in sensitivity due to changes in ion transmission and ambient water vapor. Note, the sensitivity varies by only 0.25% per percent change ambient water vapor mixing ratio when P_{H_2O}>0.2 torr. It is only in regions where P_{H_2O}<0.15, and changing on timescales faster than can be normalized by the $I(H_2O)^-$ that such contributions to uncertainty become important.

We expect that the precision of our N_2O_5 and $ClNO_2$ observations should be governed largely by counting statistics as we have already demonstrated for our acyl peroxy nitrate measurements using adjacent differences of high time resolution measurements of a calibration source. The 1σ relative precision under counting statistics is $S/\sqrt{S}$ where S is the signal count rate. For a 1 s integration and 100 pptv N_2O_5 or $ClNO_2$, we estimate a precision of 10% and 7.5% respectively under moist conditions. This precision improves with the square root of the integration time. Generally, atmospheric variability is large enough, even on 60-s timescales to be the dominant source of point-to-point variability. Indeed given the poor vertical mixing near the surface at night, very large relative changes in concentrations are possible on short timescales.

AMTD
2, 119–151, 2009

5 Field performance

We recently deployed the UW-CIMS instrument aboard the RV Knorr as part of the International Chemistry in the Arctic Lower Troposphere (ICEALOT) campaign. The measurement campaign ran from 19 March–24 April 2008 as the ship left Woods Hole, MA and traveled from the Long Island Sound to Rekjavik, Iceland via Tromso, Norway. For more information on the goals and measurement suite during this campaign please visit: http://saga.pmel.noaa.gov/Field/icealot/. Our goal was to provide high quality measurements of $ClNO_2$ and to test the performance of our N_2O_5 measurement technique side-by-side with the NOAA CaRDS instrument (Brown et al., 2002). Table 1 summarizes instrument performance during this campaign.

Prior to deployment, the UW-CIMS instrument and the NOAA CaRDS instrument made ambient measurements in Boulder, CO as part of the integration of the instruments into the shipping container that housed them on the RV Knorr. The inlet configuration for sampling both in Boulder, CO and on the Knorr consists of a virtual impactor, N_2O_5 and NO addition ports, a reducer, and a 12 m length of 6 mm OD PFA tubing into the sea container. Ambient air is sampled at ~11 slpm through a 1 cm length of 6 mm OD PFA tubing inlet on the front end of a custom built virtual impactor. Standard addition ports for N_2O_5 (6 mm) and NO (3 mm) are tied into the main sampling line via PFA fittings. Immediately following the NO addition port is a constriction which serves to drop the sampling line pressure to ~300 torr. A 12 m length of PFA tubing is used to transport the gas from the top of the sampling tower to the sea container where it is split ~1 m from the end to allow the UW-CIMS and NOAA CaRDS to sample from the same inlet simultaneously.

The top panel of Fig. 5 shows N_2O_5 mixing ratios measured by the UW-CIMS and the NOAA CaRDS in Boulder, CO the night of 26 February 2008. N_2O_5 mixing ratios increase throughout the night to 800 pptv, remain elevated throughout the night and then decay in the morning following sunrise likely due to the photolysis of NO_3 and its reaction with NO. For comparison we have included N_2O_5 mixing ratios determined

AMTD
2, 119–151, 2009

from the signal at the nitrate ion mass (i.e. Reaction R9) where we have used zero measurements determined only from NO additions. If we use zero measurements obtained from the hot stainless steel tube, the lack of agreement between the NO_3^- and the $I(N_2O_5)^-$ derived N_2O_5 mixing ratios worsens. The lower panel shows a point-by-point comparison of the data with the UW-CIMS N_2O_5 mixing ratio derived from $I(N_2O_5)^-$ and NO_3^- plotted versus that from the NOAA CaRDS. The slope of a linear least squares fit for $I(N_2O_5)^-$ is 1.02 with an R^2 of 0.990. The slope of the line changes by 2% when the intercept is allowed to vary from zero. The slope of a linear least squares fit for NO_3^- is 1.20 with an R^2 of 0.967 when forced through zero. The slope of the line changes by 20% when the intercept is allowed to vary from zero, resulting in a positive offset of 58 pptv. Even larger swings in sensitivity and background were observed at the NO_3^- *m/z* during the entire ICEALOT campaign (see Table 1 and Fig. 5). A more detailed comparison of the NOAA CaRDS and UW-CIMS N_2O_5 measurements from ICEALOT is warranted. However, it is clear that the $I(N_2O_5)^-$ cluster ion more accurately reflects the true N_2O_5 mixing ratio over the full range of atmospheric concentrations than does the NO_3^- ion.

Figure 6 shows a time series of N_2O_5 and $ClNO_2$ mixing ratios measured by the UW-CIMS during the first portion of ICEALOT. The RV Knorr left Woods Hole, MA on 19 March, headed west-southwest up the Long Island Sound until 21 March, when it reversed course, traveled east-northeast and exited the sound by 22 March. During the traverse of the Long Island Sound, the prevailing wind-direction shifted from southerly flow, bringing air influenced primarily by Long Island sources, to northwesterly flow bringing air influenced by sources in Connecticut and New York. Most nights, N_2O_5 reached 100–250 pptv with $ClNO_2$ being generally equal to or higher at mixing ratios of 150–200 pptv. Here we show a few nights where concentration maxima were 10–100 pptv, illustrating the low detection limits of this method.

During the field deployment, several tests were performed to assess the presence of interferences at the *m/z* used to detect $ClNO_2$ and the potential generation of $ClNO_2$ by reactions of N_2O_5 on inlet tubing walls. Figure 7 summarizes the results of such

AMTD
2, 119–151, 2009

tests. In the top panel, we plot the raw signal obtained at $I(^{35}ClNO_2)^-$ *m/z* versus the signal at the $I(^{37}ClNO_2)^-$ *m/z* from the entire period of sampling in the Long Island Sound (see Fig. 6). A linear least squares fit to the data (not shown), forced through the intercept, yields a slope of 0.3207 and R^2=0.996. This is within 0.5% percent of the theoretical isotopic value, 0.3199, indicated by the thick solid line. The experimental and theoretical values are well within the precision of the instrument expected for 100 ms sampling. This result provides confidence that our measurements were of a chlorine-containing species that had the same *m/z* as $ClNO_2$ and can be destroyed on hot (180C) stainless steel. We note that the signals detected at the ICl^- *m/z* did not demonstrate the expected Cl-isotopic ratio. In the lower panel of Fig. 7, we show raw signals at the $I(N_2O_5)^-$ and the $I(^{35}ClNO_2)^-$ *m/z* during a standard addition of 2.0 ppbv N_2O_5 to ambient air. The N_2O_5 was added directly to the very top of the sampling manifold, 1cm from the sampling tip, just after a full night of continuous sampling and detection of N_2O_5 and $ClNO_2$. The first addition occurs at the point labeled "a". The N_2O_5 signal responds from a background count rate of 15 Hz to 2200 Hz, yielding a UW-CIMS calibration factor for N_2O_5 of 1.1 Hz/pptv in ambient air. No change in the $ClNO_2$ signal is evident during the N_2O_5 addition confirming that production of $ClNO_2$ from N_2O_5 reactions on the tubing wall was minimal during this, and most such additions. Indeed, while the sampling manifold was cleaned almost daily, we used any evidence of $ClNO_2$ signal enhancements during N_2O_5 additions to ambient air as an indication of inlet contamination and the inlet tubing was replaced and the sampling manifold was cleaned.

6 Summary and conclusions

We report on a new method for the simultaneous in situ detection of nitryl chloride, $ClNO_2$, and N_2O_5 using chemical ionization mass spectrometry (CIMS). The novel N_2O_5 detection scheme is direct and it does not suffer from high and variable chemical interferences, which are associated with the more typical nitrate anion based approach.

We address the roles of water vapor, electric field strengths, and instrument zero determinations, which can greatly influence the overall sensitivity and detection limit of the method. The sensitivity to both N_2O_5 and $ClNO_2$ is logarithmically dependant on the partial pressure of water vapor in the ion-molecule reaction region. Under typical marine boundary layer conditions, the technique can be largely insensitive to changes in atmospheric water vapor concentrations, but under continental sampling, low water vapor concentrations could greatly reduce sensitivity. Detection of the iodide-clusters of these species has a threshold-dependence on the electric field strength in the CDC. Above ~70 V/cm at 1.5 torr in the CDC, the clusters become essentially undetectable. We demonstrate the ability for simultaneous in situ measurements of $ClNO_2$ and N_2O_5 while on board the RV Knorr as part of the ICEALOT 2008 Field Campaign. These observations serve to reinforce the importance of $ClNO_2$ as a nocturnal NO_x and Cl-atom reservoir in coastal regions. Our technique allows a way to measure both reactant (N_2O_5) and product ($ClNO_2$) of complex gas-particle chemistry with a single instrument.

Acknowledgements. William P. Dubé, Hendrik Fuchs, and Steven S. Brown provided the cavity ringdown N_2O_5 measurements for comparison. We thank National Oceanic and Atmospheric Administration (NOAA) scientists Steven S. Brown, Bill Kuster and Eric J. Williams of the Earth System Research Laboratory and Patricia K. Quinn and Timothy Bates of the Pacific Marine Environmental Laboratory for financial and logistical support during the integration and ICEALOT campaign. We greatly appreciate the efforts of the RV Knorr crew exhibited during the entire cruise. We thank V. Faye McNeill for insights into nitryl chloride detection, G. M. Wolfe for help with instrument integration prior to ICEALOT and T. H. Bertram for useful discussions about instrument performance. JPK gratefully acknowledges the Camille and Henry Dreyfus foundation for financial support through a postdoctoral fellowship.

References

Aldener, M., Brown, S. S., Stark, H., Williams, E. J., Lerner, B. M., Kuster, W. C., Goldan, P. D., Quinn, P. K., Bates, T. S., Fehsenfeld, F. C., and Ravishankara, A. R.: Reactivity and

Loss Mechanisms of NO_3 and N_2O_5 in a Polluted Marine Environment: Results from in situ Measurements during New England Air Quality Study 2002, J. Geophys. Res.-Atmos., 111, D23S73, doi:10.1029/2006JD007252, 2006.

Arsene, C., Bougiatioti, A., Kanakidou, M., Bonsang, B., and Mihalopoulos, N.: Tropospheric OH and Cl levels deduced from non-methane hydrocarbon measurements in a marine site, Atmos. Chem. Phys., 7, 4661–4673, 2007, http://www.atmos-chem-phys.net/7/4661/2007/.

Atkinson, R.: Atmospheric Chemistry of VOCs and NOx, Atmos. Environ., 34, 2063–2101, 2000.

Ayers, J. D. and Simpson, W. R.: Measurements of N_2O_5 near Fairbanks, Alaska, J. Geophys. Res.-Atmos., 111, D14309, doi:10.1029/2006JD007070, 2006.

Behnke, W., George, C., Scheer, V., and Zetzsch, C.: Production and Decay of $ClNO_2$ from the Reaction of Gaseous N_2O_5 with NaCl solution: Bulk and Aerosol Experiments, J. Geophys. Res.-Atmos., 102, 3795–3804, 1997.

Bertram, T. H., Riedel, T. P., and Thornton, J. A.: An Experimental Technique for the Direct Measurement of Heterogeneous and Multiphase Reactions on Ambient Particles: Application to N_2O_5 reactivity, Atmos. Chem. Phys. Discuss., submitted, 2009.

Brown, S. S., Dubé, W. P., Osthoff, H. D., Stutz, J., Ryerson, T. B., Wollny, A. G., Brock, C. A., Warneke, C., De Gouw, J. A., Atlas, E., Neuman, J. A., Holloway, J. S., Lerner, B. M., Williams, E. J., Kuster, W. C., Goldan, P. D., Angevine, W. M., Trainer, M., Fehsenfeld, F. C., and Ravishankara, A. R.: Vertical Profiles in NO_3 and N_2O_5 Measured from an Aircraft: Results from the NOAA P-3 and Surface Platforms during the New England Air Quality Study 2004, J. Geophys. Res.-Atmos., 112, D22304, doi:10.1029/2007JD008883, 2007.

Brown, S. S., Neuman, J. A., Ryerson, T. B., Trainer, M., Dubé, W. P., Holloway, J. S., Warneke, C., de Gouw, J. A., Donnelly, S. G., Atlas, E., Matthew, B., Middlebrook, A. M., Peltier, R., Weber, R. J., Stohl, A., Meagher, J. F., Fehsenfeld, F. C., and Ravishankara, A. R.: Nocturnal Odd-Oxygen Budget and its Implications for Ozone Loss in the Lower Troposphere, Geophys. Res. Lett., 33, L08801, doi:10.1029/2006GL025900, 2006.

Brown, S. S., Stark, H., Ciciora, S. J., McLaughlin, R. J., and Ravishankara, A. R.: Simultaneous in situ Detection of Atmospheric NO_3 and N_2O_5 via Cavity Ring-Down Spectroscopy, Rev. Sci. Instrum., 73, 3291–3301, 2002.

Cavender, A. E., Biesenthal, T. A., Bottenheim, J. W., and Shepson, P. B.: Volatile organic compound ratios as probes of halogen atom chemistry in the Arctic, Atmos. Chem. Phys., 8,

1737–1750, 2008,
http://www.atmos-chem-phys.net/8/1737/2008/.
Dentener, F. J. and Crutzen, P. J.: Reaction of N_2O_5 on Tropospheric Aerosols – Impact on the Global Distributions of NOx, O_3, and OH, J. Geophys. Res.-Atmos., 98, 7149–7163, 1993.
Evans, M. J. and Jacob, D. J.: Impact of new Laboratory Studies of N_2O_5 Hydrolysis on Global Model Budgets of Tropospheric Nitrogen Oxides, Ozone, and OH, Geophys. Res. Lett., 32, L09813, doi:10.1029/2005GL022469, 2005.
Finlayson-Pitts, B. J., Ezell, M. J., and Pitts, J. N.: Formation of Chemically Active Chlorine Compounds by Reactions of Atmospheric NaCl Particles with Gaseous N_2O_5 and $ClONO_2$, Nature, 337, 241–244, 1989.
Fuchs, H., Dubé, W. P., Cicioira, S. J., and Brown, S. S.: Determination of Inlet Transmission and Conversion Efficiencies for in situ Measurements of the Nocturnal Nitrogen Oxides, NO_3, N_2O_5 and NO_2, via Pulsed Cavity Ring-Down Spectroscopy, Anal. Chem., 80, 6010–6017, 2008.
Geyer, A., Alicke, B., Mihelcic, D., Stutz, J., and Platt, U.: Comparison of Tropospheric NO_3 Radical Measurements by Differential Optical Absorption Spectroscopy and Matrix Isolation Electron Spin Resonance, J. Geophys. Res.-Atmos., 104, 26097–26105, 1999.
Harrison, A. G.: Chemical Ionization Mass Spectrometry, CRC Press, Boca Raton, Fla., 1983.
Heintz, F., Platt, U., Flentje, H., and Dubois, R.: Long-term Observation of Nitrate Radicals at the Tor Station, Kap Arkona (Rugen), J. Geophys. Res.-Atmos., 101, 22891–22910, 1996.
Huey, L. G.: Measurement of Trace Atmospheric Species by Chemical Ionization Mass Spectrometry: Speciation of Reactive Nitrogen and Future Directions, Mass Spectrom. Rev., 26, 166–184, 2007.
Huey, L. G., Hanson, D. R., and Howard, C. J.: Reactions of SF_6^- and I^- with Atmospheric Trace Gases, J. Phys. Chem., 99, 5001–5008, 1995.
Jacob, D. J.: Heterogeneous Chemistry and Tropospheric Ozone, Atmos. Environ., 34, 2131–2159, 2000.
Logan, J. A.: Tropospheric Chemistry – A Global Perspective, Abstracts of Papers of the American Chemical Society, 182, 78-PHYS, 1981.
McNeill, V. F., Patterson, J., Wolfe, G. M., and Thornton, J. A.: The effect of varying levels of surfactant on the reactive uptake of N_2O_5 to aqueous aerosol, Atmos. Chem. Phys., 6, 1635–1644, 2006,
http://www.atmos-chem-phys.net/6/1635/2006/.

Mentel, T. F., Bleilebens, D., and Wahner, A.: A Study of Nighttime Nitrogen Oxide Oxidation in a Large Reaction Chamber - The Fate of NO_2 N_2O_5, HNO_3, and O_3 at Different Humidities, Atmos. Environ., 30, 4007–4020, 1996.

Noxon, J. F., Norton, R. B., and Marovich, E.: NO_3 in the Troposphere, Geophys. Res. Lett., 7, 125–128, 1980.

Osthoff, H. D., Roberts, J. M., Ravishankara, A. R., Williams, E. J., Lerner, B. M., Sommariva, R., Bates, T. S., Coffman, D., Quinn, P. K., Dibb, J. E., Stark, H., Burkholder, J. B., Talukdar, R. K., Meagher, J., Fehsenfeld, F. C., and Brown, S. S.: High Levels of Nitryl Chloride in the Polluted Subtropical Marine Boundary Layer, Nature Geoscience, 1, 324–328, 2008.

Pechtl, S. and von Glasow, R.: Reactive Chlorine in the Marine Boundary Layer in the Outflow of Polluted Continental Air: A Model Study, Geophys. Res. Lett., 34, L11813, doi:10.1029/2007GL029761, 2007.

Platt, U., Allan, W., and Lowe, D.: Hemispheric average Cl atom concentration from $^{13}C/^{12}C$ ratios in atmospheric methane, Atmos. Chem. Phys., 4, 2393–2399, 2004, http://www.atmos-chem-phys.net/4/2393/2004/.

Platt, U. and Heintz, F.: Nitrate Radicals in Tropospheric Chemistry, Israel J. Chem., 34, 289–300, 1994.

Simpson, W. R.: Continuous Wave Cavity Ring-Down Spectroscopy Applied to in situ Detection of Dinitrogen Pentoxide (N_2O_5), Rev. Sci. Instrum., 74, 3442–3452, 2003.

Slusher, D. L., Huey, L. G., Tanner, D. J., Flocke, F. M., and Roberts, J. M.: A Thermal Dissociation-Chemical Ionization Mass Spectrometry (TD-CIMS) Technique for the Simultaneous Measurement of Peroxyacyl Nitrates and Dinitrogen Pentoxide, J. Geophys. Res.-Atmos., 109, D19315, doi:10.1029/2004JD004670, 2004.

Smith, N., Plane, J. M. C., Nien, C. F., and Solomon, P. A.: Nighttime Radical Chemistry in the San-Joaquin Valley, Atmos. Environ., 29, 2887–2897, 1995.

Spicer, C. W., Chapman, E. G., Finlayson-Pitts, B. J., Plastridge, R. A., Hubbe, J. M., Fast, J. D., and Berkowitz, C. M.: Unexpectedly High Concentrations of Molecular Chlorine in Coastal Air, Nature, 394, 353–356, 1998.

Stutz, J., Alicke, B., Ackermann, R., Geyer, A., White, A., and Williams, E.: Vertical Profiles of NO_3, N_2O_5, O_3, and NOx in the Nocturnal Boundary Layer: 1. Observations during the Texas Air Quality Study 2000, J. Geophys. Res.-Atmos., 109, D16399, doi:10.1029/2004JD005217, 2004.

Thornton, J. A. and Abbatt, J. P. D.: N_2O_5 Reaction on Submicron Sea Salt Aerosol: Kinetics,

Products, and the Effect of Surface Active Organics, J. Phys. Chem. A, 109, 10004–10012, 2005.
Thornton, J. A., Braban, C. F., and Abbatt, J. P. D.: N_2O_5 Hydrolysis on Sub-Micron Organic Aerosols: the Effect of Relative Humidity, Particle Phase, and Particle Size, Phys. Chem. Chem. Phys., 5, 4593–4603, 2003.
van Aardenne, J. A., Carmichael, G. R., Levy, H., Streets, D., and Hordijk, L.: Anthropogenic NOx Emissions in Asia in the Period 1990–2020, Atmos. Environ., 33, 633–646, 1999.
Veres, P., Roberts, J. M., Warneke, C., Welsh-Bon, D., Zahniser, M., Herndon, S., Fall, R., and de Gouw, J.: Development of Negative-Ion Proton-Transfer Chemical-Ionization Mass Spectrometry (NI-PT-CIMS) for the Measurement of Gas-Phase Organic Acids in the Atmosphere, Int. J. Mass Spectrom., 274, 48–55, 2008.
Wayne, R. P., Barnes, I., Biggs, P., Burrows, J. P., Canosamas, C. E., Hjorth, J., Lebras, G., Moortgat, G. K., Perner, D., Poulet, G., Restelli, G., and Sidebottom, H.: The Nitrate Radical - Physics, Chemistry, and the Atmosphere, Atmos. Environ. Part A-General Topics, 25, 1–203, 1991.
Wolfe, G. M., Thornton, J. A., McNeill, V. F., Jaffe, D. A., Reidmiller, D., Chand, D., Smith, J., Swartzendruber, P., Flocke, F., and Zheng, W.: Influence of trans-Pacific pollution transport on acyl peroxy nitrate abundances and speciation at Mount Bachelor Observatory during INTEX-B, Atmos. Chem. Phys., 7, 5309–5325, 2007, http://www.atmos-chem-phys.net/7/5309/2007/.
Wood, E. C., Wooldridge, P. J., Freese, J. H., Albrecht, T., and Cohen, R. C.: Prototype for in situ detection of Atmospheric NO_3 and N_2O_5 via Laser-Induced Fluorescence, Environ. Sci. Technol., 37, 5732–5738, 2003.
Yienger, J. J.: An Evaluation of Chemistry's Role in the Winter-Spring Ozone Maximum found in the Northern Midlatitude Free Troposphere, J. Geophys. Res.-Atmos., 104, 8329–8329, 1999.
Zhu, R. S. and Lin, M. C.: Ab initio Studies of ClOx Reactions: Prediction of the Rate Constants of ClO+NO for the Forward and Reverse Processes, Chem. Phys. Chem., 5, 1864–1870, 2004.

Table 1. Summary of UW-CIMS performance for simultaneous, in situ detection of N_2O_5 and $ClNO_2$ during ICEALOT.

Species	Ion	Sensitivity (Hz/pptv)	Background (Hz)	Detection Limit[a] (pptv) (1 s/1 min)	Zero Uncertainty[b] (pptv)
N_2O_5	$I(N_2O_5)^-$	0.93±0.2	2.1±2	11.0/2.7	2.3
N_2O_5	NO_3^-	4–40[c]	200–4000[c]	<2[c]	50–100[c]
$ClNO_2$	$I(ClNO_2)^-$	1.18±0.15	2.7±2.3	13.0/3.0	2.0

[a] Mixing ratio which yields an instantaneous signal-to-noise ratio of 2:1. This theoretical value assumes the background count rate is known with absolute certainty.
[b] Based on 1σ variation between adjacent background measurements. This value is a more realistic measure of the lowest detectable mixing ratio. See text for details.
[c] Sensitivity and background values for NO_3^- *m/z* covaried unpredictably, and thus these values are highly uncertain.

AMTD
2, 119–151, 2009

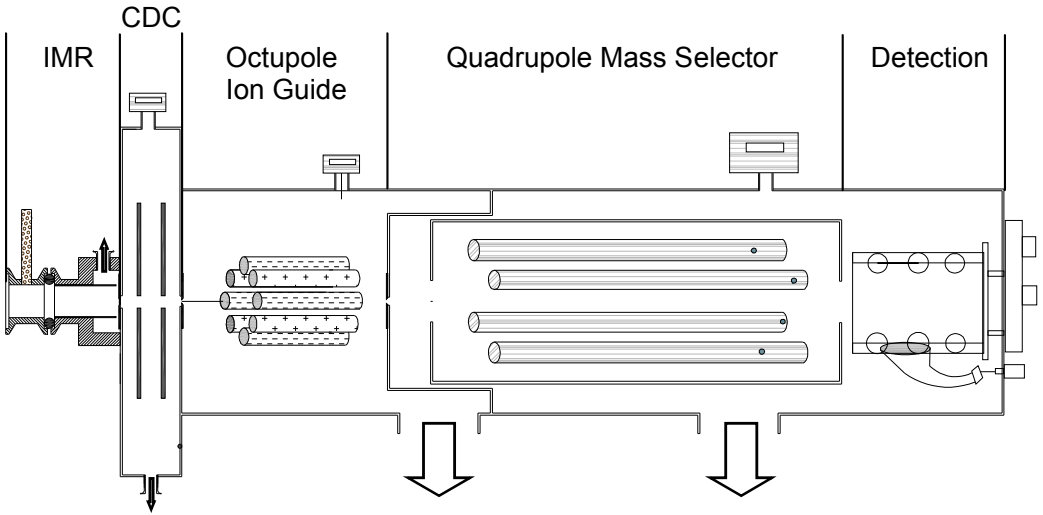

Fig. 1. Schematic of the University of Washington Chemical Ionization Mass Spectrometer (UW-CIMS). IMR ≡ ion molecule region; CDC ≡ collisional dissociation chamber; QMS ≡ quadrupole mass spectrometer.

AMTD
2, 119–151, 2009

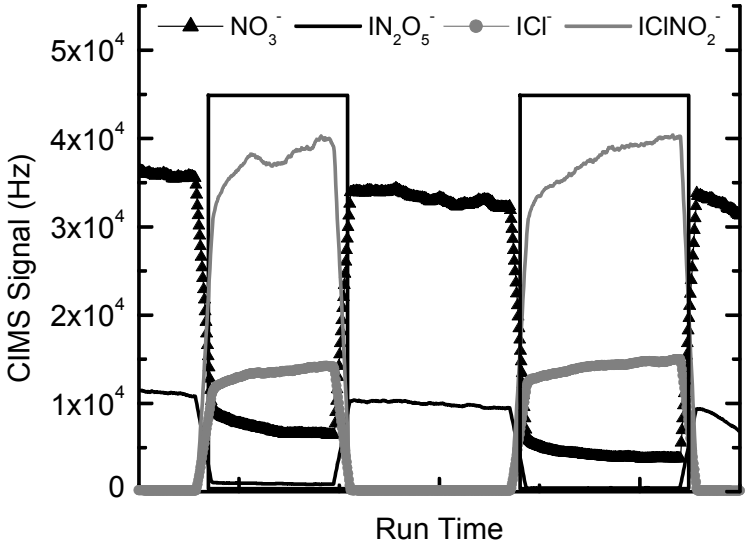

Fig. 2. UW-CIMS ion time trace showing the evolution of the ICl^- (solid grey circles), $I(ClNO_2)^-$ (grey line), $I(N_2O_5)^-$ (black line) and NO_3^- (solid black triangles) anions when sampling a trace amount (750 pptv) of N_2O_5. The boxed regions highlight sampling periods during which the N_2O_5 flow was exposed to a wet NaCl salt bed prior to sampling by the UW-CIMS.

AMTD
2, 119–151, 2009

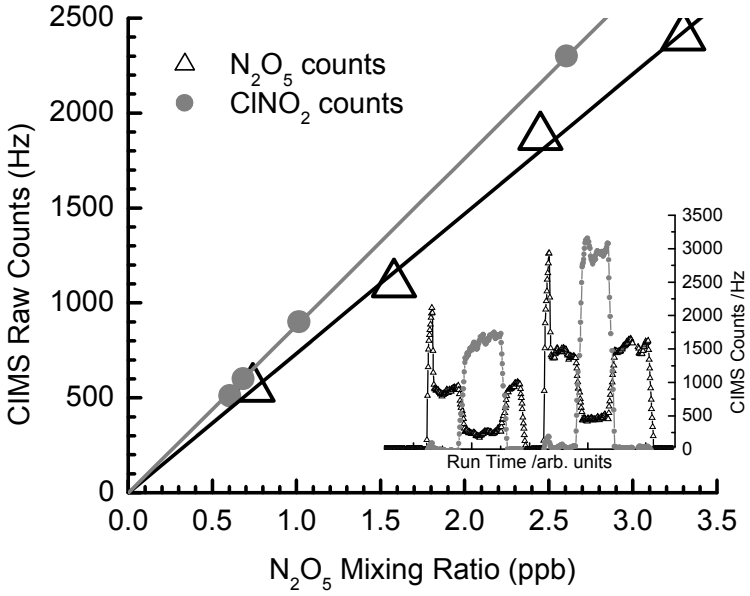

Fig. 3. UW-CIMS signal (Hz) vs mixing ratio (ppbv) for N_2O_5 (triangles) and $ClNO_2$ (circles) at the $I(N_2O_5)^-$ and $I(ClNO_2)^-$ cluster anion masses, respectively. The size of the points corresponds to the 1σ deviation of the points used in the average. The N_2O_5 mixing ratio was determined using the NOAA CaRDS. The $ClNO_2$ mixing ratio is assumed to be equal to the amount of N_2O_5 which reacts over a wet NaCl salt bed. The slopes of the linear regressions provide the UW-CIMS sensitivities to each cluster anion.

AMTD
2, 119–151, 2009

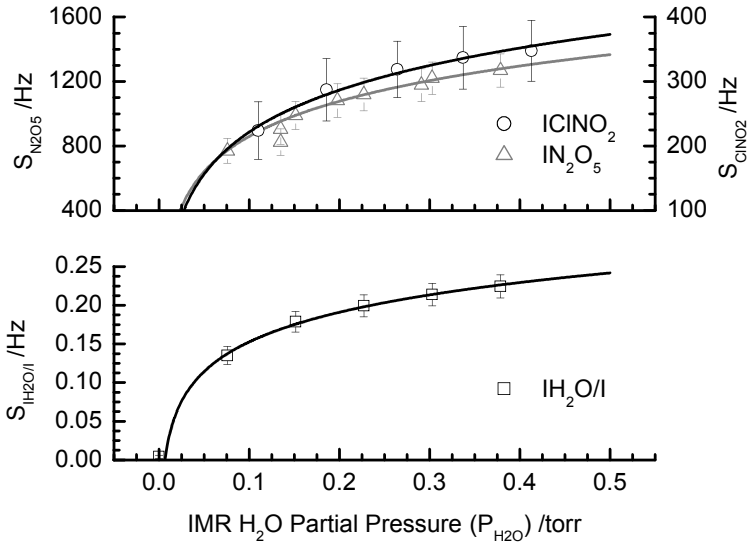

Fig. 4. Upper Panel: UW-CIMS cluster anion signal dependence on the ion molecule region (IMR) water partial pressure (P_{H_2O}). Lower Panel: The iodide-water (IH_2O^-) cluster anion signal, normalized to the iodide reagent ion signal (I^-).

AMTD
2, 119–151, 2009

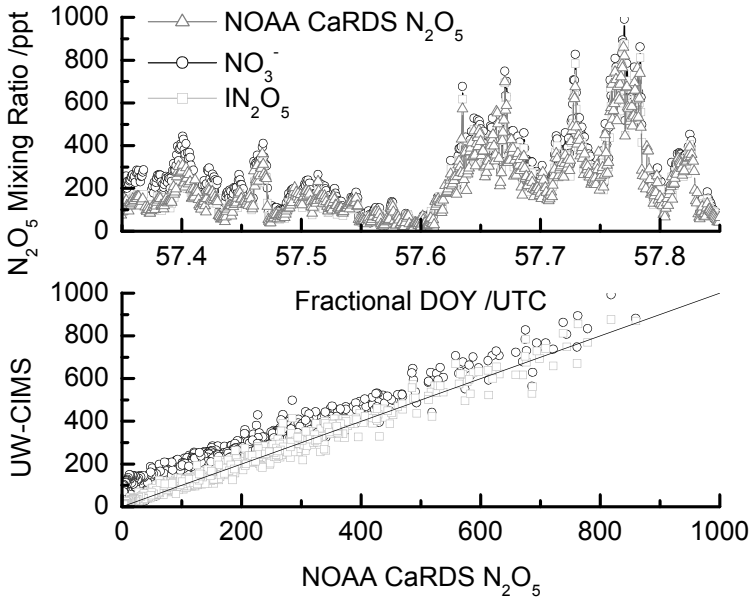

Fig. 5. Top Panel: The N_2O_5 mixing ratio for February 26^{th}, 2008, as measured by the NOAA CaRDS (triangles), the $I(N_2O_5)^-$ cluster (squares) and NO_3^- (circles). Lower Panel: A comparison between the $I(N_2O_5)^-$ cluster (squares) and NO_3^- anion (circles) with the NOAA cavity ringdown measurement, respectively. The solid black line is a 1:1 ratio.

AMTD
2, 119–151, 2009

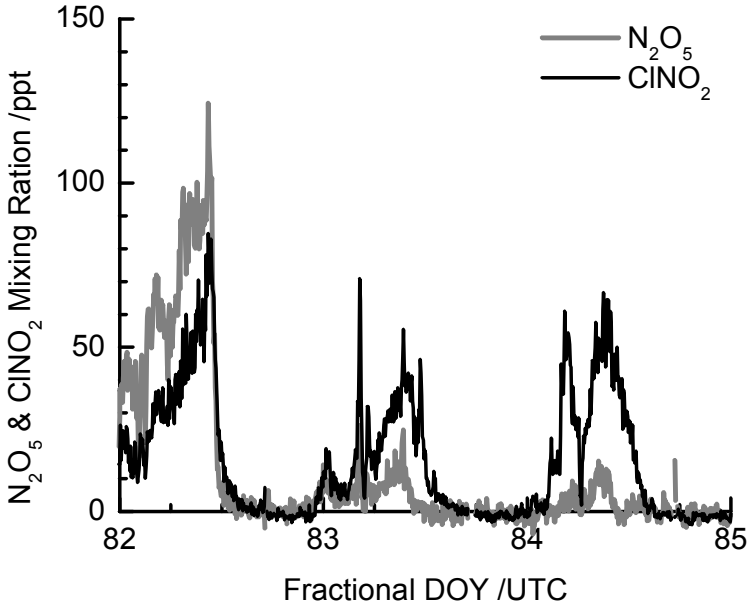

Fig. 6. The $ClNO_2$ (black) and N_2O_5 (grey) mixing ratios measured from 22 March (DOY 82) through 24 March 2008 during the ICEALOT field campaign. The maximum N_2O_5 mixing ratio was ~100 pptv on 22 March (82), while $ClNO_2$ reached 80 pptv.

AMTD
2, 119–151, 2009

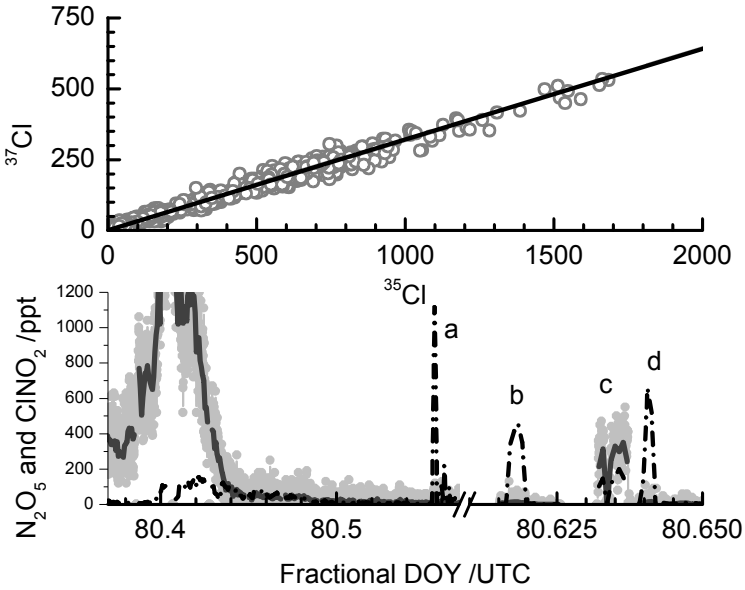

Fig. 7. Top Panel: The measured $ClNO_2$ isotope ratio (open circles) and a linear fit (m=0.320, R^2=0.996). Lower Panel: Time trace of N_2O_5 (black dashed line), $ClNO_2$ (grey) and 1-min binned average $ClNO_2$ (dark grey) mixing ratios for 20 March 2008. **(a)** Standard addition of 1.02 ppbv of N_2O_5 to the ambient sample flow. **(b)** Standard addition of ~500 pptv of N_2O_5 to the ambient sample bypassing a wet NaCl salt bed. **(c)** Standard addition of ~500 pptv of N_2O_5 to ambient sample flow which passes over the wet NaCl salt bed. **(d)** Standard addition of 700 pptv of N_2O_5 to the ambient sample flow bypassing the NaCl salt bed.

AMTD
2, 119–151, 2009